17th International Conference on
Flow Processes in Composites Materials (FPCM17)
Sheffield, United Kingdom, 30 June to 02 July 2026.

TITLE: In-situ Optical Fibre Sensing for Validation of a Thermo-Chemo-Mechanical Residual Stress Model in Thick Composite Laminates

AUTHOR(S): Anastasia P. Tsavea[1], Samuel Furtado[2], James M. Maguire[1], Colin Robert[3], Edward D. McCarthy[4], Kevin Kerrigan[2], Conchúr M. Ó Brádaigh[3]

AFFILIATION(S):

[1]University of Sheffield, School of Mechanical, Aerospace and Civil Engineering, Sheffield, S1 3JD, UK

[2]Advanced Manufacturing Research Centre, University of Sheffield, Sheffield, S60 5TZ, UK

[3]University of Sheffield, School of Chemical, Materials and Biological Engineering, Sheffield, S1 3JD, UK

[4]School of Engineering, Institute for Materials and Processes, The University of Edinburgh, The King's Buildings, Edinburgh, EH9 3FB, United Kingdom

ABSTRACT:

Reactive thermoplastic resins such as Elium® enable recyclable, room-temperature infusion of large composite structures (Figure 1), but thick-section processing (>50-100 mm) remains potentially limited by process-induced residual stresses, warpage and damage. In thick laminates, exothermic polymerisation generates pronounced through-thickness gradients in temperature and degree of conversion, driving spatially and temporally varying chemical shrinkage and stiffness evolution (skin-core effects and inside-out polymerisation). These coupled gradients control when and where stresses become locked-in, and can lead to severe dimensional instability, but more importantly in the case of thick sections used in wind and tidal stream blades, affect the fatigue life of those components. Maduro [1] reported that reducing residual stresses by half can triple the cycles to failure of wind turbine blades, underscoring the importance of process design and in-situ monitoring for these applications.

A coupled thermo-chemo-mechanical model has been developed to predict residual stress development in thick E-glass/Elium® 191 XO/SA laminates, with the longer-term aim of enabling process optimisation and manufacturability assessment for recyclable wind and tidal blade sub-structures [2]. The model is implemented in Abaqus/Standard using coupled temperature-displacement elements (Figure 2) and user subroutines to resolve cure kinetics, internal heat generation, thermal and chemical strains, and gelation-dependent stiffness evolution. Polymerisation is captured in the Abaqus user subroutine USDFLD via an autocatalytic, diffusion-limited kinetic law, while the HETVAL subroutine computes the associated exothermic heat generation. UEXPAN defines thermal expansion and chemical shrinkage from micromechanics, and UMAT implements a Cure-Hardening Instantaneously Linear Elastic (CHILE) formulation with a gelation criterion, such that stresses are negligible prior to gelation and evolve elastically thereafter. The laminate considered is a 200 × 200 mm unidirectional panel with 60 plies (52.95 mm thick), discretised with a structured through-thickness-refined mesh (approximately 70,000 nodes) on one-sided tooling with convective heat loss at the free surface. Numerical case studies comparing ambient consolidation at 20 °C with a modest thermal intervention based on 30 °C forced convection applied to the exposed surface until peak exotherm demonstrate strong process sensitivity. Chemical shrinkage is the dominant driver of residual stress build-up, and the thermal intervention reduces maximum spring-back by 33% (13.4 mm to 9.0 mm) and peak tensile stresses by up to 65% (for example, σ_{11} from 25.8 MPa to 9.0 MPa), while reversing the global warpage mode from U-shape to ∩-shape (Figure 3). These results indicate that through-thickness temperature and conversion gradients do not simply scale residual stresses, but shift the relative timing of stiffness development and shrinkage through the thickness, which can alter the stress distribution qualitatively and invert the resulting distortion mode.

Through-thickness embedded thermocouple measurements from infusion trials were used to characterise exotherm magnitude and timing and to calibrate the thermal-kinetic part of the model [3]; however, temperature-only data cannot resolve internal strain evolution. Here, in-situ optical fibre sensing is used to generate internal strain and temperature histories that can be compared directly against coupled FE predictions, in both ambient and elevated temperature case studies through the use of heated silicone mats.

The measurements target (i) internal strain versus time at multiple through-thickness locations, (ii) at least one reliable internal temperature measurement, and (iii) separation of chemical shrinkage and thermal expansion from stiffness evolution to support constitutive benchmarking (CHILE versus viscoelastic formulations).

A hybrid sensing architecture combines long- and short-tailed fibre Bragg gratings (otherwise referred to as FBGs, seen in Figure 4), and distributed fibre-optic sensing (DFOS) embedded within the laminate. Long-tailed FBGs are treated as "true laminate strain" sensors by selecting gauge length and embedding conditions that give near-unity strain transfer (strain transfer coefficient $\eta_{\mathrm{long}} \approx 1$), so $\varepsilon_{\mathrm{laminate}}(t) \approx \varepsilon_{\mathrm{long}}(t)$. Long-tailed gratings are positioned at distinct depths (near-surface, upper-mid, mid-plane, lower-mid and tool-side) to capture $\varepsilon(z,t)$ through thickness during consolidation. In parallel, a short-tailed FBG is embedded near the mid-plane to intentionally introduce imperfect strain transfer via shear-lag, such that $\varepsilon_{\mathrm{short}}(t) = \eta(C(t))\, \varepsilon_{\mathrm{laminate}}(t)$. Here $\eta(C(t))$ is a cure-dependent strain-transfer coefficient governed by the evolving matrix shear stiffness and the fibre/coating geometry. The ratio $\frac{\varepsilon_{\mathrm{short}}(t)}{\varepsilon_{\mathrm{long}}(t)} \approx \eta(C(t))$ enables property inversion during cure, following the short-gauge shear-lag approach reported by Minakuchi [4] for polymerising systems. As the matrix shear stiffness increases during cure, strain transfer improves and η increases towards unity, so the short-tailed FBG response converges towards the laminate strain measured by the long-tailed FBG. This allows inversion for (1) directional chemical shrinkage strain versus time/degree of cure (in-plane transverse, and potentially through thickness with vertical embedding), (2) the evolving matrix modulus $E_m(a)$ or an apparent modulus proxy), and (3) direction-dependent effective thermal expansion behaviour, without relying on interrupted-cure mechanical testing, which is impractical for Elium® systems.

DFOS is acquired using a Luna ODiSI 6100 Rayleigh-based optical frequency domain reflectometry (OFDR) system, providing millimetre-scale spatial resolution along the entire length of embedded fibre-optic paths, which has been previously used for in-situ VARTM flow front tracking [5]. This methodology resolves localised strain gradients associated with skin-core polymerisation mismatch, free-edge/boundary-layer effects and evolving constraint, and enables mapping from fibre-optic length to physical laminate coordinates. To account for the temperature-sensitive Rayleigh measurements, and to isolate mechanically driven strain accumulation, results from embedded strain-compensated distributed optical fibre temperature sensors will also be considered. Embedding layouts include optimised in-plane serpentine-like routing (Figure 5) to sample multiple regions and through-thickness ramps to reconstruct $\varepsilon(z,t)$ directly. Measurements span the full process window (8-12 h acquisition, peak at approximately 3 h and cooling thereafter), under maximum temperatures below 100 °C. The combined FBG and Luna-OFDR dataset (Figure 6) is then used to separate thermal expansion from chemical-shrinkage-driven strain development throughout polymerisation and subsequent cooling. Sensor layout is designed with interrogation constraints in mind (FBG spectral shift under high strain, grating density to avoid peak collision, channel synchronisation) and with minimum bend radii of 25 mm for embedded fibre routing in thick laminates.

The resulting dataset enables direct benchmarking of through-thickness strain histories $\varepsilon(z,t)$ against thermo-chemo-mechanical FE predictions, identification of the onset and progression of stress locking relative to gelation and conversion gradients, and quantitative comparison between conservative CHILE predictions and viscoelastic formulations that capture post-gel stress relaxation. By combining distributed and discrete optical fibre measurements with coupled process modelling, the study resolves internal strain mechanisms that control warpage and residual stress in thick infusible thermoplastic laminates. It also provides a basis for targeted thermal management and processing strategies to reduce skin-core mismatch and manufacturing-induced defects in recyclable composite structures.

References

[1] M. A. Miranda Maduro, *Influence of Curing Cycle on the Build-up of Residual Stresses and the Effect on the Mechanical Performance of Fibre Composites*. Risø, Roskilde, Denmark: DTU Wind Energy, 2021.

[2] A. P. Tsavea *et al.*, 'Modelling Residual Stresses In Thick-section Thermoplastic Composites For Wind And Tidal Energy Blades', presented at the 24th International Conference on Composite Materials, Baltimore, Maryland USA, 2025.

[3] A. Tsavea *et al.*, 'Validation Of A Thermochemical Model For Thick- Section Thermoplastic Composite Infusions', presented at the SAMPE Europe 2025, Amsterdam, The Netherlands, 2025.

[4] S. Minakuchi, ‘In situ characterization of direction-dependent cure-induced shrinkage in thermoset composite laminates with fiber-optic sensors embedded in through-thickness and in-plane directions’, *J. Compos. Mater.*, vol. 49, no. 9, pp. 1021–1034, Apr. 2015, doi: 10.1177/0021998314528735.

[5] J. Davidson *et al.*, ‘Distributed Fibre Optic Sensing for Real-Time Monitoring of VARTM Manufacturing and Processing of Composite Laminates’, Jan. 2025. doi: 10.13140/RG.2.2.14264.87040.

Figure 1 An Elium®-based wind turbine blade, manufactured by the ZEBRA project

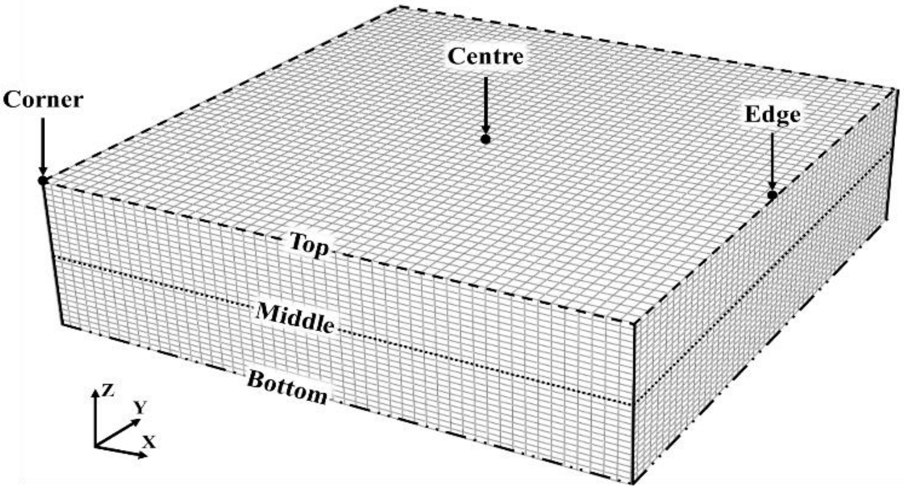

Figure 2 ABAQUS simulation setup using temperature-displacement coupled brick elements

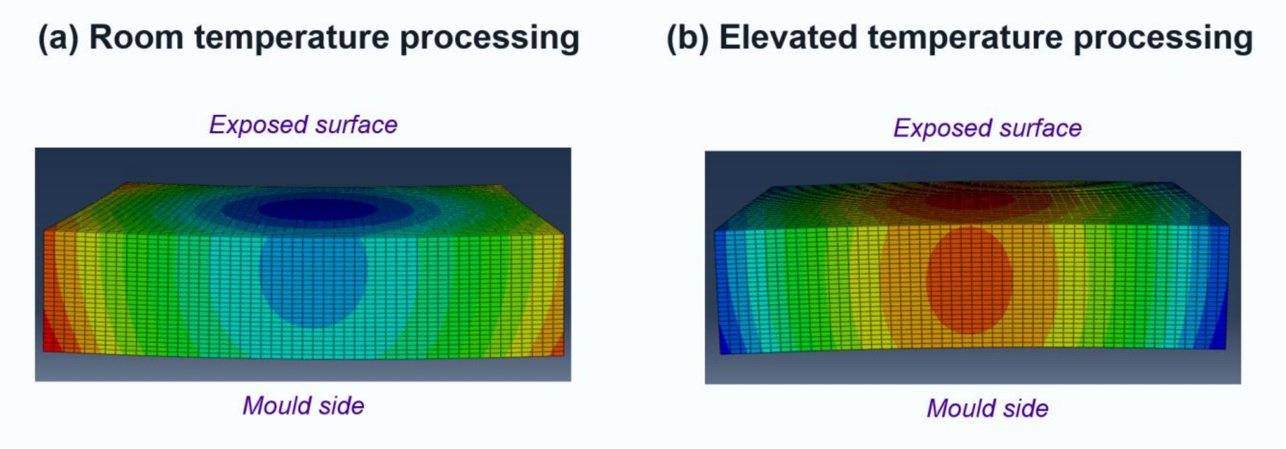

Figure 3 Deformation mode change as a result of elevated temperature processing

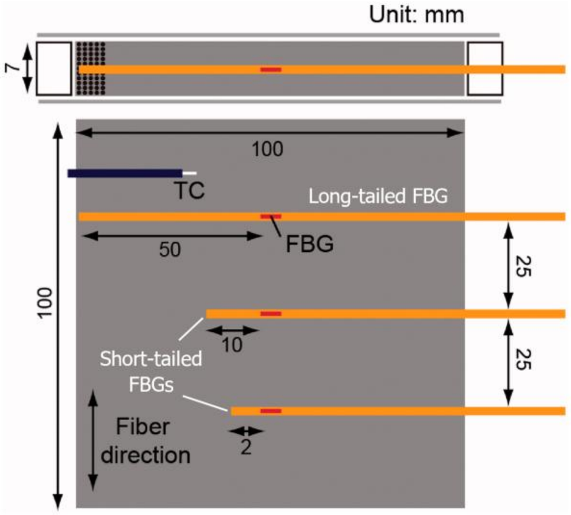

Figure 4 Long- and short-tailed FBG implementation as presented by Minakuchi [4]

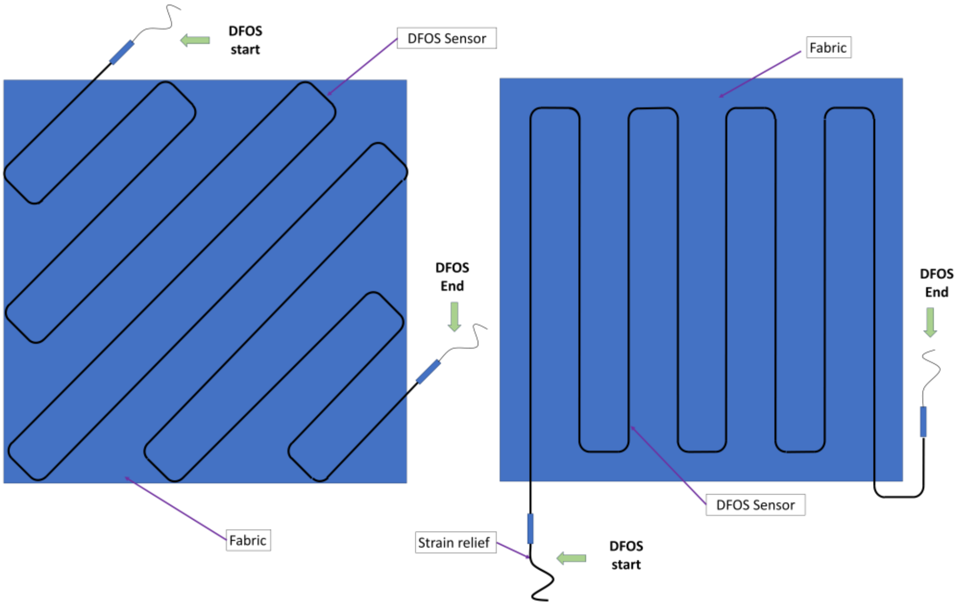

Figure 5 DFOS routing layout schematic (Left: Parallel to infusion flow front; Right; 45° to infusion flow front)

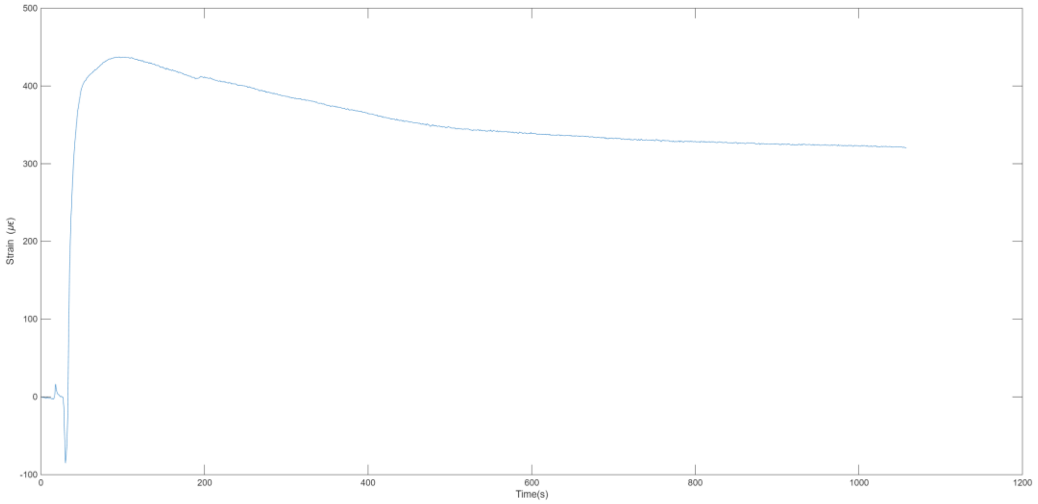

Figure 6 Example of Luna results (strain at specific point over time)

The abstract should (a) address **at least one of the core themes**, (b) not exceed two A4 pages of text, and (c) not exceed two further sides of A4 for Figures/Tables